Scanning Microscopy Vol. 11, 1997 (Pages 335-344) 0891-7035/97$5.00+.25
Scanning Microscopy International, Chicago (AMF O'Hare), IL 60666 USA

ELECTRON HOLOGRAPHY AND LORENTZ MICROSCOPY OF MAGNETIC THIN FILMS AND MULTILAYERS

M.R. McCartney[1,*] and David J. Smith[1,2]

[1]Center for Solid State Science, and [2]Department of Physics and Astronomy, Arizona State University, Tempe, AZ

Abstract

A recently acquired 200-kV field emission gun transmission electron microscope equipped with a high-magnification Lorentz lens, an electrostatic biprism, and a slow-scan charge-coupled device (CCD) camera has been utilized for micromagnetic studies of ultrathin films and multilayers under relatively field-free conditions. For plan-view imaging of a thin Fe film and cross-sectional imaging of anisotropic FePt alloys, Lorentz microscopy and off-axis electron holography provide useful complementary information. However, Lorentz out-of-focus (Fresnel) microscopy has limited applicability for ultrathin layers because of overlapping contrast due to Fresnel fringes. For multilayers with very small bilayer periods ($\leq$ 3 nm), undersampling becomes a serious problem for off-axis electron holography and alternative phase reconstruction algorithms will need to be investigated.

Key Words: Electron holography, Lorentz microscopy, thin films, magnetic materials, magnetic fields, magnetization.

*Address for correspondence:
M.R. McCartney
Center for Solid State Science
Arizona State University
Tempe, AZ 85287-1704

Telephone number: (480) 965-4558
FAX number: (480) 965-9004
E-mail: molly.mccartney@asu.edu

Introduction

Following the recent trends in computer hardware, the utility of future magnetic devices will lie in their capacity for higher storage density, which will necessitate further reductions in the size of information blocks, with simultaneous down-scaling of the distances between adjacent blocks. Obvious problems in fabrication will arise. First, the micromagnetic structure will become comparable in dimensions to the mean bit size. Second, the high net magnetization within individual bits will cause mutual interaction by way of their inherent leakage fields. In order to optimize the overall performance of devices based on magnetic materials, techniques are needed to investigate micromagnetic structure at the highest possible resolution.

Electron holography has long been used to provide images of electrostatic and magnetic potentials in and around materials (for recent reviews of earlier work see, for example, Lichte, 1991; Tonomura, 1993). Phase shifts imposed on the electron wavefront by these potentials can in principle be utilized to give quantitative two-dimensional mapping of these fields. For magnetic materials, alternate electron microscopy techniques include Fresnel and Foucault imaging, and differential phase contrast (DPC) imaging with segmented detectors in the scanning transmission electron microscope (STEM) (Chapman *et al*., 1993). Due to the necessity of imaging magnetic materials in a field-free region to prevent magnetization saturation, the spatial resolution of these techniques has historically been restricted to 10 nm or more (McFadyen and Chapman, 1992).

In this work, we report our recent studies of magnetic thin films and multilayers by electron holography and Lorentz microscopy using a transmission electron microscope (TEM) with a low-field objective lens and additional mini-lenses located near the sample (Chapman *et al*., 1993). This combination of technique and instrument allows for direct magnetic field characterization to the nanometer scale. Magnetic materials that will be described include multilayer films which display giant magnetoresistance (GMR), thin film alloys with pronounced out-of-plane magnetic fields intended for longitudinal magnetic recording (LMR), and nanometer-scale thin films. We also discuss related image processing problems which

include the separation of phase shifts due to electrostatic potentials from those due to magnetic fields, the effects of fringing magnetic fields, the loss of holographic fringe contrast for materials with large phase gradients, and the possible advantages of alternative methods for recording holograms and reconstructing the image wave.

Examination of Magnetic Materials

Successful imaging of inherent micromagnetic structure within the electron microscope requires that the sample should be located in a region effectively free of magnetic fields. Thus, either the sample must be relocated from the vicinity of the objective lens pole-pieces where typical fields can be as high as 2T or else the objective lens must be switched off. The second option is preferable since the possibilities for conventional imaging and microanalysis without shifting the specimen are still retained.

In previous generations of electron microscopes, the diffraction lenses have been operated at comparatively low excitation to provide images of magnetic specimens. Without the objective lens, the total magnification of most imaging systems is then limited in this configuration to perhaps 4000x, and because of poor aberration coefficients the attainable resolution might only be 10 nm. These limitations of magnification and resolution can be overcome to a large extent by the incorporation of a strong mini-lens into the lower bore of the objective lens pole-piece (Chapman *et al*., 1993).

There are two primary mechanisms in a TEM for achieving useful micromagnetic image contrast: both take advantage of the so-called Lorentz force which occurs whenever an electron beam passes through a region with transverse magnetic fields. Strongly defocussed images show lines of dark and light contrast at magnetic domain walls due to the sideways deflection of the electron beam (Chapman, 1984). Alternatively, off-axis electron holograms will reveal phase changes due to fields within the sample, as described by the following equation (Reimer, 1989), where it is also assumed that the sample is suitably tilted to avoid strong diffracting conditions (see Figure 1):

$$\Delta\phi = C_E V_0 t + \frac{e}{\hbar} \int_{AB} \int_{CD} \mathbf{B} \bullet d\mathbf{A} \qquad (1)$$

V_0 is the mean inner potential, t is the specimen thickness, ABCD is the surface defined by the paths of the object and reference beams, and B_n is the component of the magnetic field normal to the electron beam direction. This equation can be re-written as

$$\Delta\phi = C_E V_0 t + e B_n s \frac{t}{\hbar} \qquad (2)$$

For a sample of constant thickness and composition, the first term can be omitted, viz.,

$$\frac{\Delta\phi}{\Delta s} = e B_n \frac{t}{\hbar} \qquad (3)$$

Thus, the slope of the phase is proportional to the normal component of the magnetic field within the sample, i.e., regions of constant *slope* correspond to constant magnetic field.

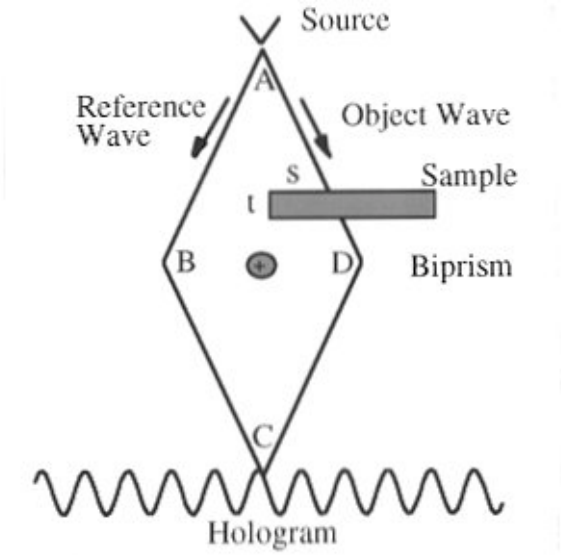

Figure 1. Schematic illustration of path integral used for calculating magnetic phase shift.

Experimental Details

A Philips CM200 TEM equipped with a thermally-assisted field-emission gun (FEG) electron source (Mul *et al.*, 1990) was used for the observations reported below. An additional (Lorentz) mini-lens just below the lower objective lens pole-piece enables image magnifications of up to about 70 000x to be obtained on the charge-coupled device (CCD) camera with the objective lens power supply turned off. Using this mini-lens, we have demonstrated point resolutions of less than 3.0 nm, as shown by diffractogram analysis, and we have resolved lattice fringes with a spacing of 1.0 nm. An electrostatic biprism in the selected area aperture plane was used for generating off-axis electron holograms. All images and holograms were recorded digitally with a commercial 1024x1024 pixel, multi-scan CCD camera (Gatan 694; Gatan, Pleasanton, CA) for convenience in subsequent image processing. Several types of magnetic materials were evaluated in this study - relevant details of each sample are given in the following sections. Preparation for TEM examination in cross-section involved standard procedures including mechanical polishing and ion-beam

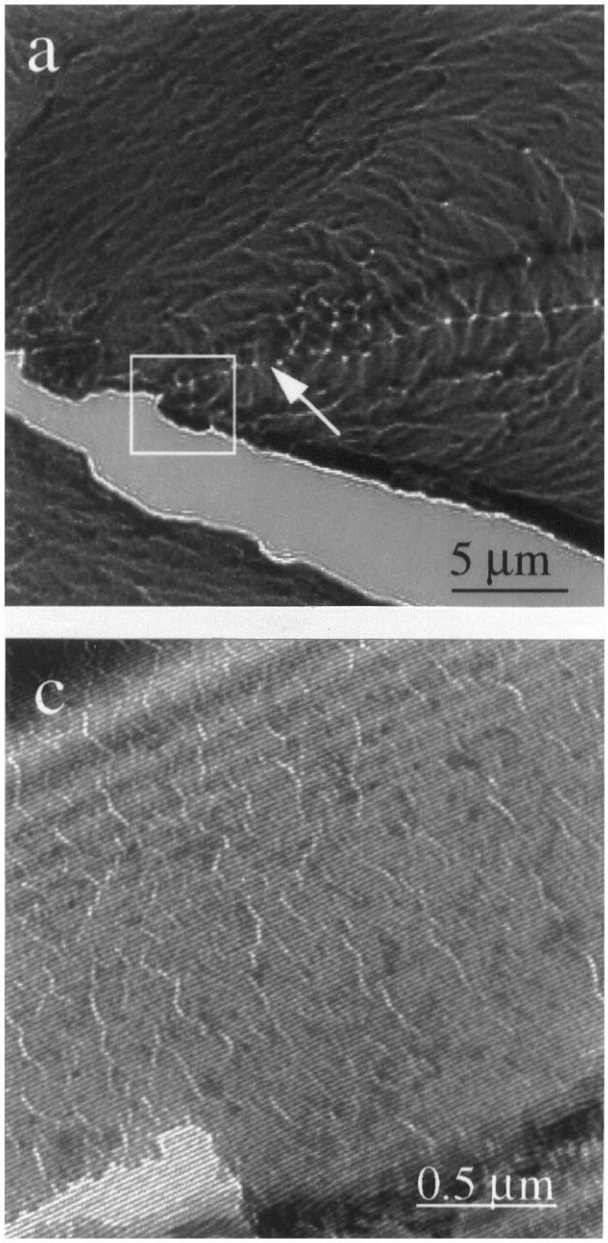

Figure 2. (**a**) Low-magnification, out-of-focus, Lorentz image of thin Fe film recorded at an original magnification of about 3,750x; (**b**) Higher magnification image from part of area shown in Figure 2a; (**c**) Electron hologram from area indicated in Figure 2b.

milling (Ar^+, 5 keV, 12-14°) to perforation. All images and holograms were recorded at an accelerating voltage of 200 kV.

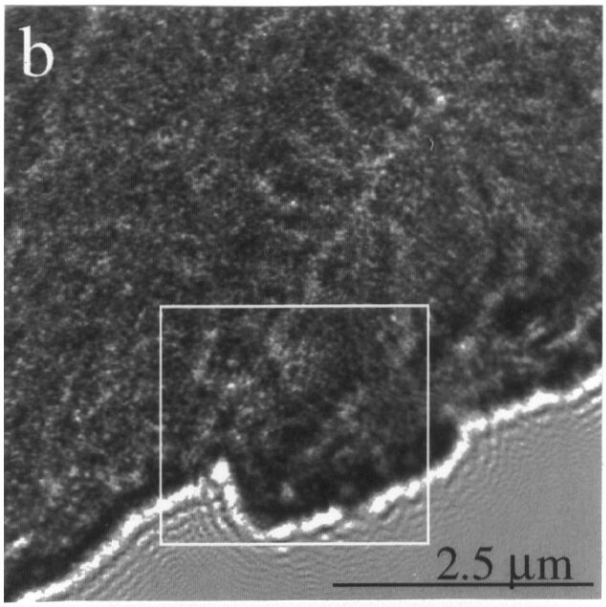

Results

Thin Fe film

In order to provide an initial indication of the capabilities of the new microscope, we first studied an evaporated Fe film with a thickness of about 30 nm.

Figure 2a shows a defocussed Fresnel micrograph recorded with the CCD camera at an imaging magnification of about 3750x, which is close to the traditional TEM magnification limit for Lorentz imaging. The bright line (arrowed) corresponds to a domain wall boundary, and some magnetization ripple is also visible. A higher magnification Fresnel image of the delineated region at somewhat less defocus is shown in Figure 2b. The extensive Fresnel fringe pattern visible at the sample edge is a direct consequence of the high lateral coherence of the illumination resulting from the field emission gun (FEG) electron source. The presence of similar fringes around other image features could clearly obscure finer magnetic contrast. An electron hologram from the edge of the Fe film, near part of the domain wall visible in Figure 2a, is shown enlarged in Figure 2c. The holographic interference fringes are clearly visible running laterally across the image from the bottom left. Bright string-like features in the hologram correspond to grain boundaries or micro-cracks in the film. No reference holograms of the vacuum wave to correct for distortions of the phase were used for any of the examples shown in this paper. This was due either to the absence of nearby vacuum regions or unacceptable shifting of the fringe pattern upon moving the sample out of the field of view. The consequences of this lack of correction will be considered in the discussion section.

The hologram was otherwise processed in standard

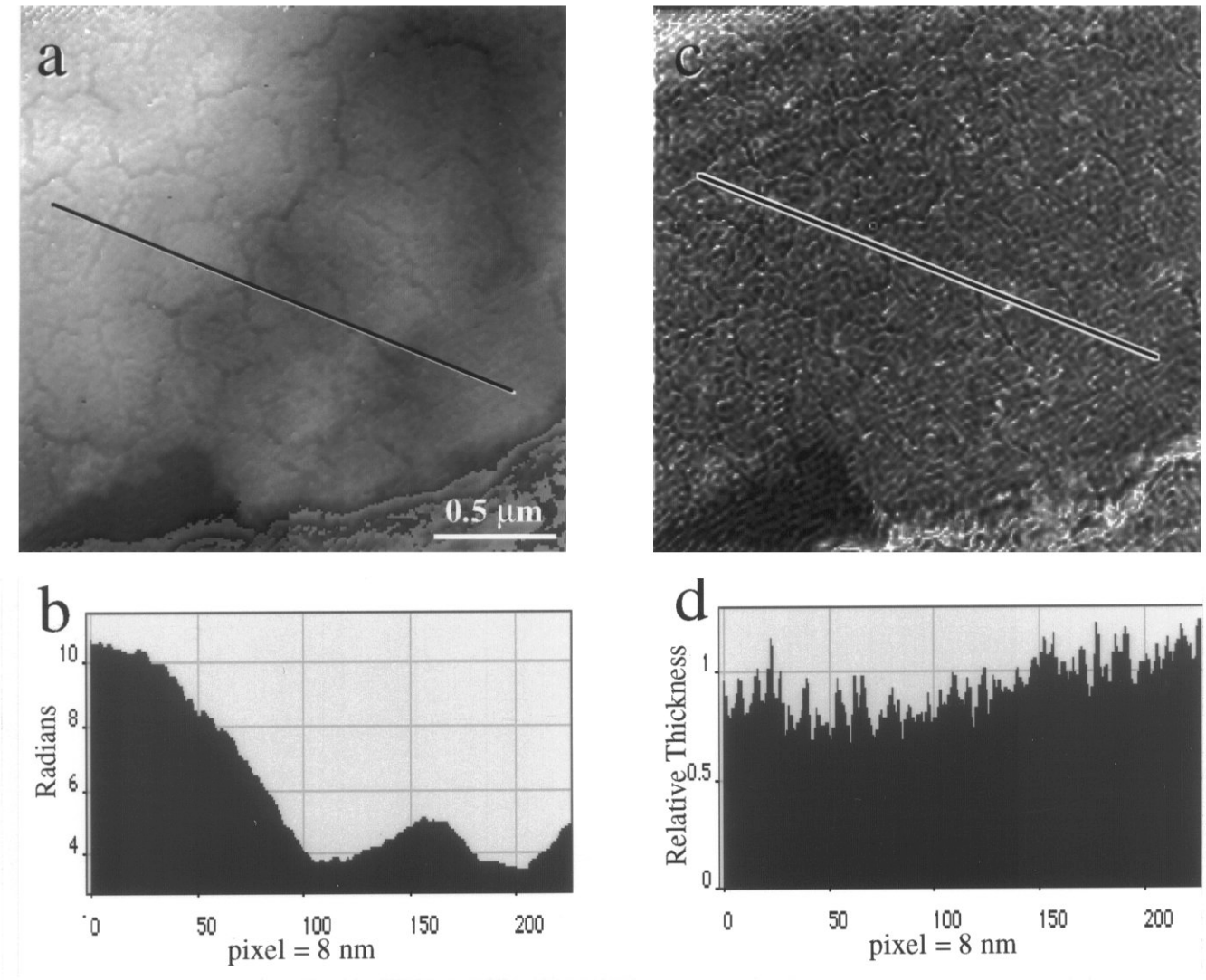

Figure 3. (**a**) Reconstructed phase image of Fe film from hologram shown in Figure 2c; (**b**) line trace from phase image; (**c**) relative thickness image after normalization using the amplitude image; (**d**) line trace from relative thickness image.

fashion by first executing a Fourier transform, followed by an inverse Fourier transformation applied to one of the sidebands only. The resulting phase image is shown in Figure 3a. In this phase image, regions of constant slope correspond to regions of constant magnetic field so that the domain walls appear as areas where the slope of the phase image is changing. In particular, the bright ridge region on the left side of Figure 3a is the domain wall which appears dark in the underfocus image of Figure 2a. Similarly, the bright domain wall lines and other bright features in Figure 2a appear as dark valleys in Figure 3a. Since the effect of the domain wall on the phase is of particular interest, a ten pixel averaged line scan was taken as indicated, and the result is shown in Figure 3b. However, according to Equation (2), before this trace can be interpreted in terms of the magnetic field alone, it must first be verified that variations in the specimen normalized specimen thickness was calculated from the thickness do not account for the changes. Thus, the amplitude image using the procedure developed elsewhere (McCartney and Gajdardziska-Josifovska, 1993), and the result is shown in Figure 3c. A further trace was taken along the same line of the sample as in Figure 3a, and the result is shown in Figure 3d. From this trace, it is clear that changes in the specimen thickness do not correlate with the observed phase changes. In regions where the specimen is thicker, i.e., on the lower right hand side of the image and line scan, the phase is decreasing rather than increasing as expected from the mean inner

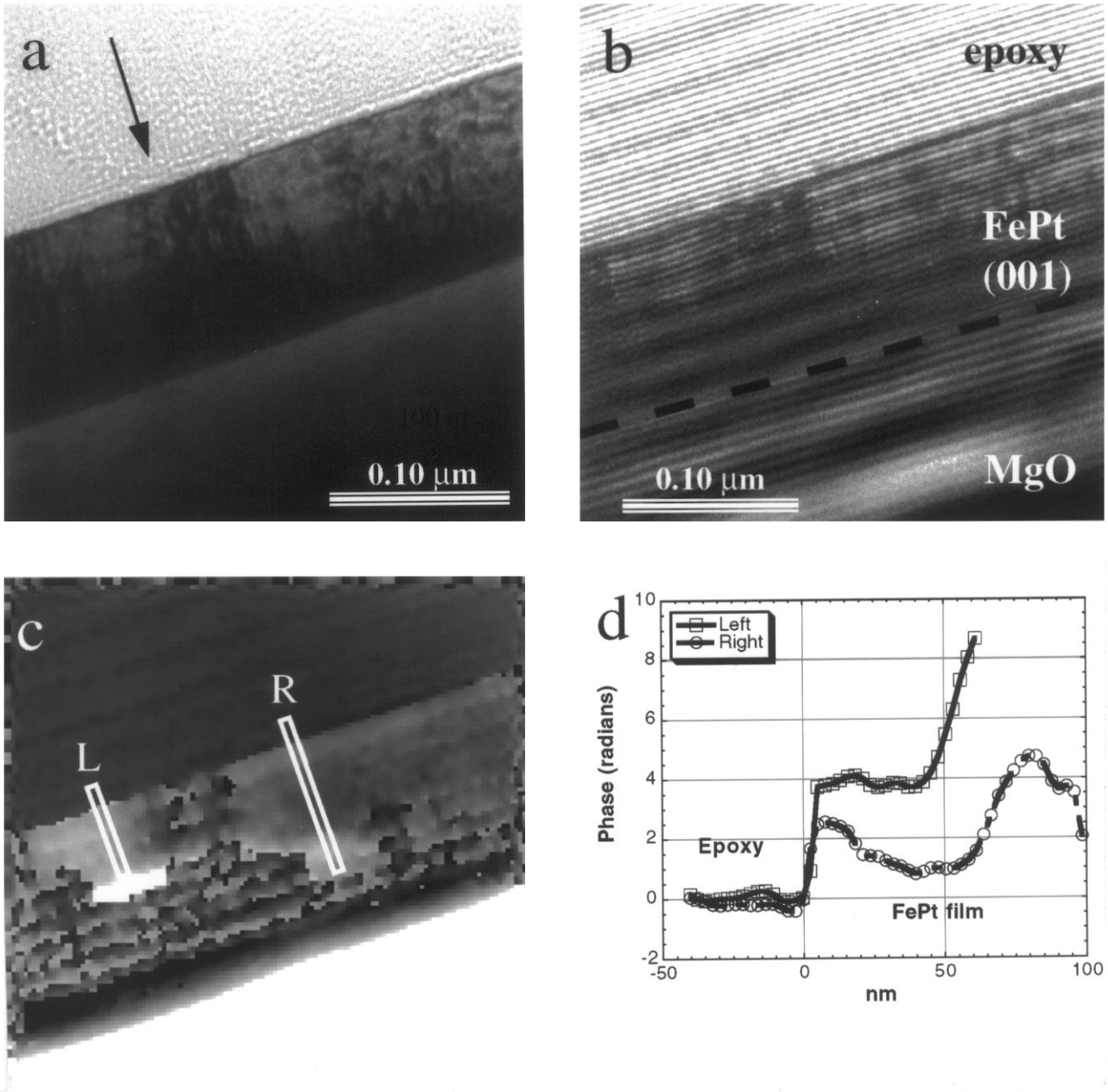

Figure 4. (**a**) In-focus image recorded with Lorentz mini-lens showing defective region in epitaxial FePt alloy film grown with easy axis in-plane; (**b**) corresponding electron hologram from same area as Figure 4a; (**c**) reconstructed phase image; (**d**) line traces from areas indicated on Figure 4c.

potential. Hence, in accordance with Equation (3), the changes in slope visible in Figure 3b must be due primarily to changes in the local magnetic field. Complications from phase changes due to the leakage field can be estimated from the curvature of the phase in vacuum. In this case, none is detectable and so it does not interfere with the above qualitative analysis of the magnetization state of the film. It is clear that the extra magnification and the clarity of the in-focus image would allow for the unambiguous identification of areas of interest such as cross-tie walls for further chemical or high-resolution examination.

Anisotropic FePt alloy

Epitaxial layers of Fe_xPt_{1-x} ($x \sim 0.5$) alloy films, which are prospective candidates for perpendicular recording, were grown with typical thicknesses of ~100nm using the technique of molecular beam epitaxy, with co-evaporation of Fe and Pt onto MgO single-crystal substrates of (011)

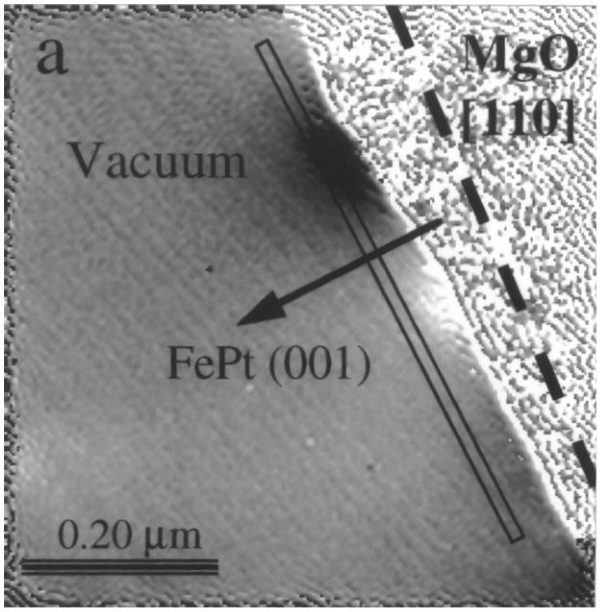

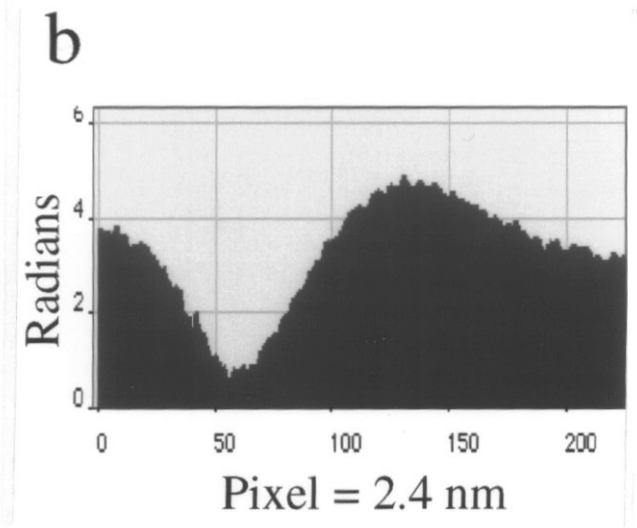

Figure 5. (**a**) Reconstructed phase image of FePt alloy film grown with easy axis parallel to film normal; (**b**) Corresponding line trace showing phase variations in vacuum outside sample due to magnetic flux leakage.

and (001) orientations using thin Pt buffer layers (Farrow *et al.*, 1996). Perpendicular or in-plane orientation of the "easy" c-axis was achieved by appropriate selection of the substrate normal. Observations in cross-section by high-resolution electron microscopy [JEM-4000EX (Jeol, Tokyo, Japan), 400 kV] confirmed the overall high quality epitaxial growth but some widely spaced regions with structural defects were also observed. Lorentz microscopy and electron holography later established that similar defective areas were generally associated with local perturbations in the magnetic field within the thin films. Electron holography of the sample

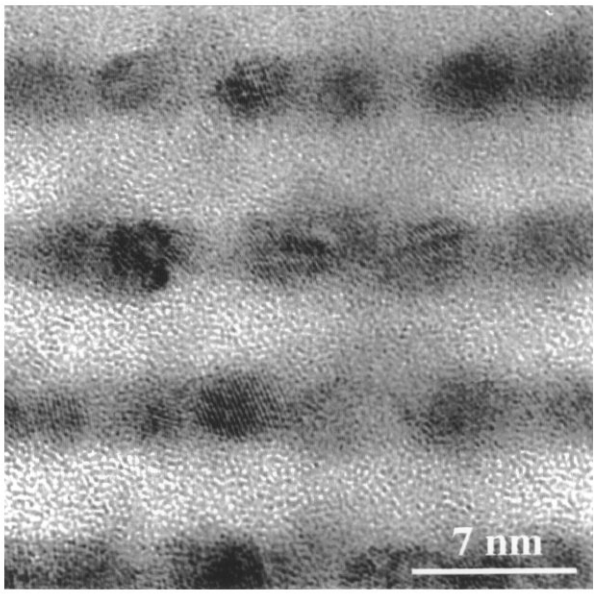

Figure 6. High resolution image showing microstructure of Co/SiO_2 multilayer.

having its easy axis parallel to the electron beam only gave phase shifts that were consistent with the mean inner potential of the two materials, i.e., the phase gradients in both the FePt film and the MgO substrate were relatively flat and positive with increased distance away from the sample edge, which is an indication of increasing specimen thickness only. Figure 4a shows an in-focus image taken with the Lorentz mini-lens where the easy axis of the FePt film is in-plane - note the region of defects arrowed - and Figure 4b shows an electron hologram from the same area. The corresponding reconstructed phase image is shown in Figure 4c, and two line traces from the marked areas are shown in Figure 4d. Parts of these traces near the MgO/FePt interface have been deliberately left incomplete because of uncertainty in phase associated with disappearance of the holographic fringes. However, the significant differences close to the film edge for the two traces are consistent with differences in the in-plane component of the magnetic field on either side of the structural defect visible in Figure 4a. On the right hand side of the image, the magnetization of the film is such that it shifts the phase in an opposite sense to that expected from the mean inner potential. That is, it points from the lower left to the upper right. From about the middle of the film to the substrate on the left hand side of the image where the phase becomes bright and then subsequently undefined, the magnetization is such that it increases the phase strongly, thus indicating an approximate reversal of the magnetization. While this difference might be due to thickness variations in the film, the uniformity in thickness of the MgO substrate at the interface would

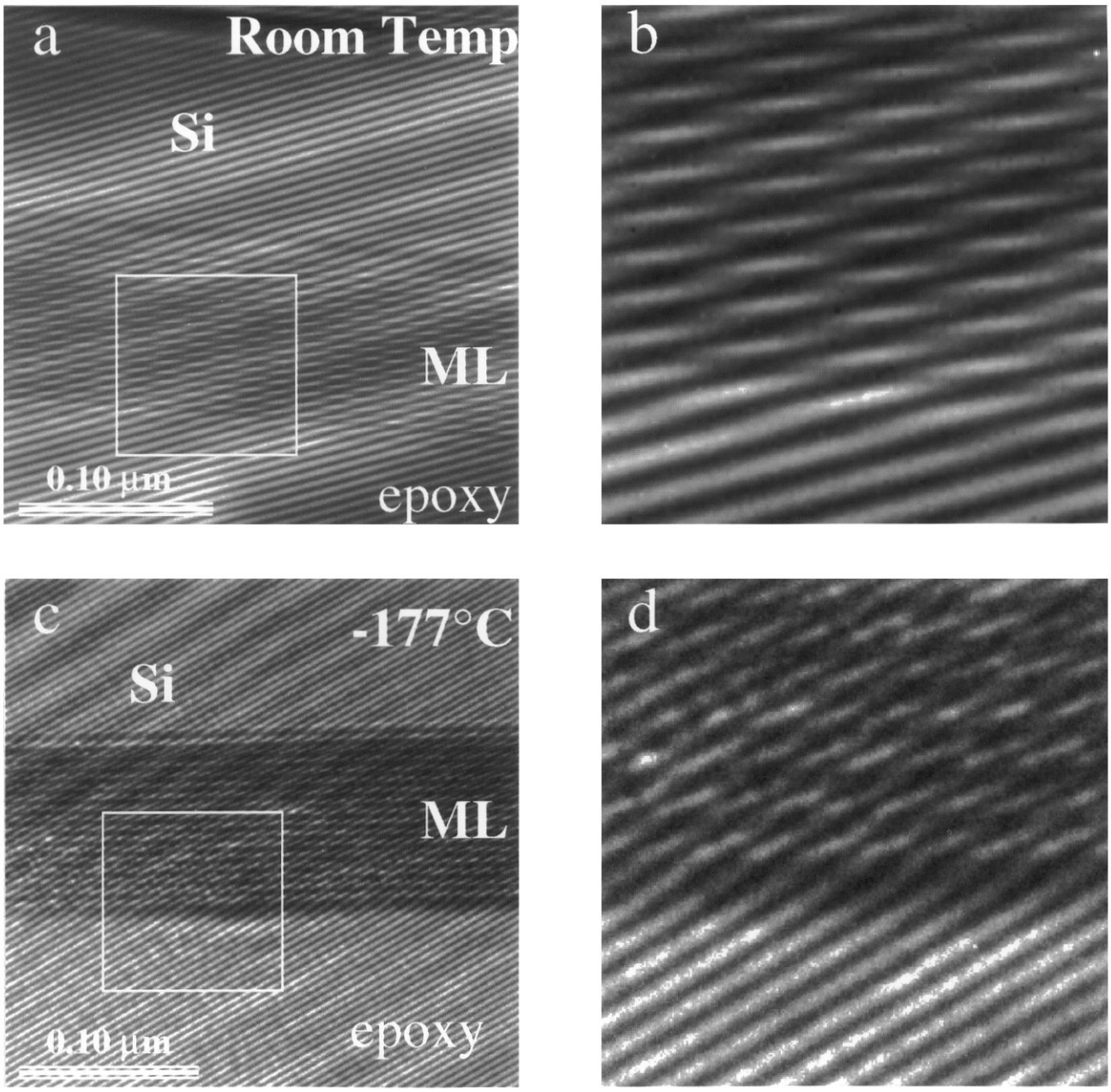

Figure 7. (**a**) electron hologram of Co/SiO_2 multilayer grown on Si substrate recorded at room temperature; (**b**) enlargement of (a); (**c**) electron hologram of Co/SiO_2 multilayer recorded at liquid nitrogen temperature; (**d**) enlargement of (**c**). Note local variations in bending of fringes.

indicate that the phase shifts are due to magnetic effects.

Finally, as shown by the reconstructed phase image in Figure 5a and the line trace in Figure 5b, observations with the FePt (001) easy axis parallel to the film normal showed variations in phase shifts in the vacuum outside the sample which indicated flux leakage along the film normal, with the upper (dark) area interpreted to point into the film and the lower (light) area to point away from the film surface. This is consistent with magnetic measurements which indicate that the film has no remanent field.

Paramagnetic Co/SiO_x multilayers

Thin Co layers embedded in an amorphous SiO_2 matrix were known to be super-paramagnetic at room temperature but magnetic at lower temperatures (Sankar,

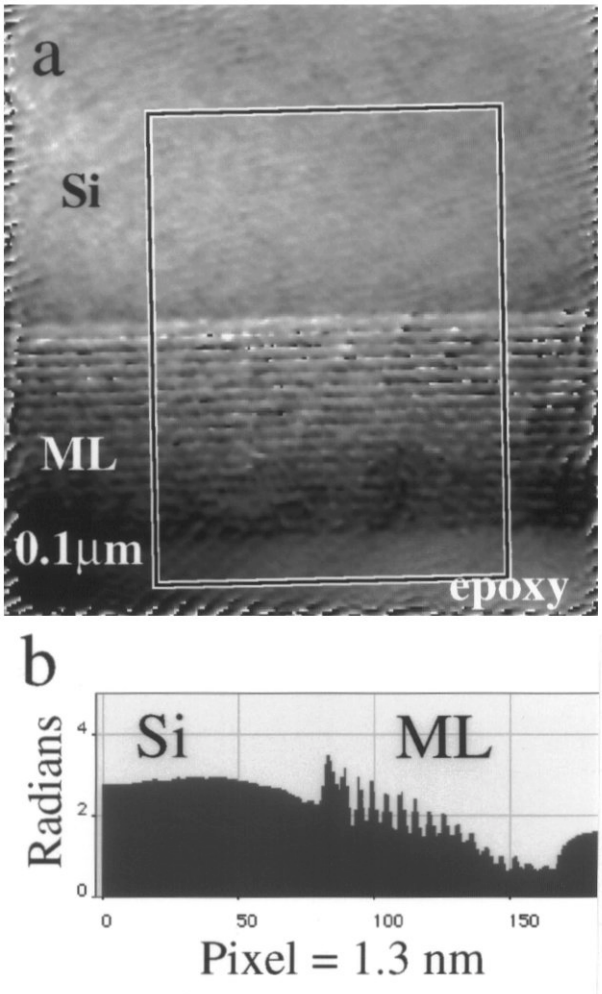

Figure 8. (**a**) reconstructed phase image of discontinuous Co/SiO_2 multilayer at liquid nitrogen temperature; (**b**) corresponding line trace from phase image.

unpublished results). Figure 6 shows a high-resolution image from part of a typical 16-layer sample recorded at room temperature, and Figures 7a and 7c show holograms from the same sample recorded at room temperature and liquid nitrogen temperature, respectively (enlargements in Figures 7b and 7d, respectively). The discontinuity of the fringes in Figure 7b is at first sight disconcerting but, since the sample is super-paramagnetic at room temperature, the magnetization directions should be reversing direction continually during the period of the exposure i.e., since the magnetic field is not constant, no measurement is possible. The variable fringe modulations visible in Figure 7d are, however, explicable in terms of fixed magnetization directions within the small, randomly aligned Co grains in the liquid nitrogen cooled sample. Figure 8a shows the reconstructed phase image of the cooled Co/SiO_2 multilayer from the

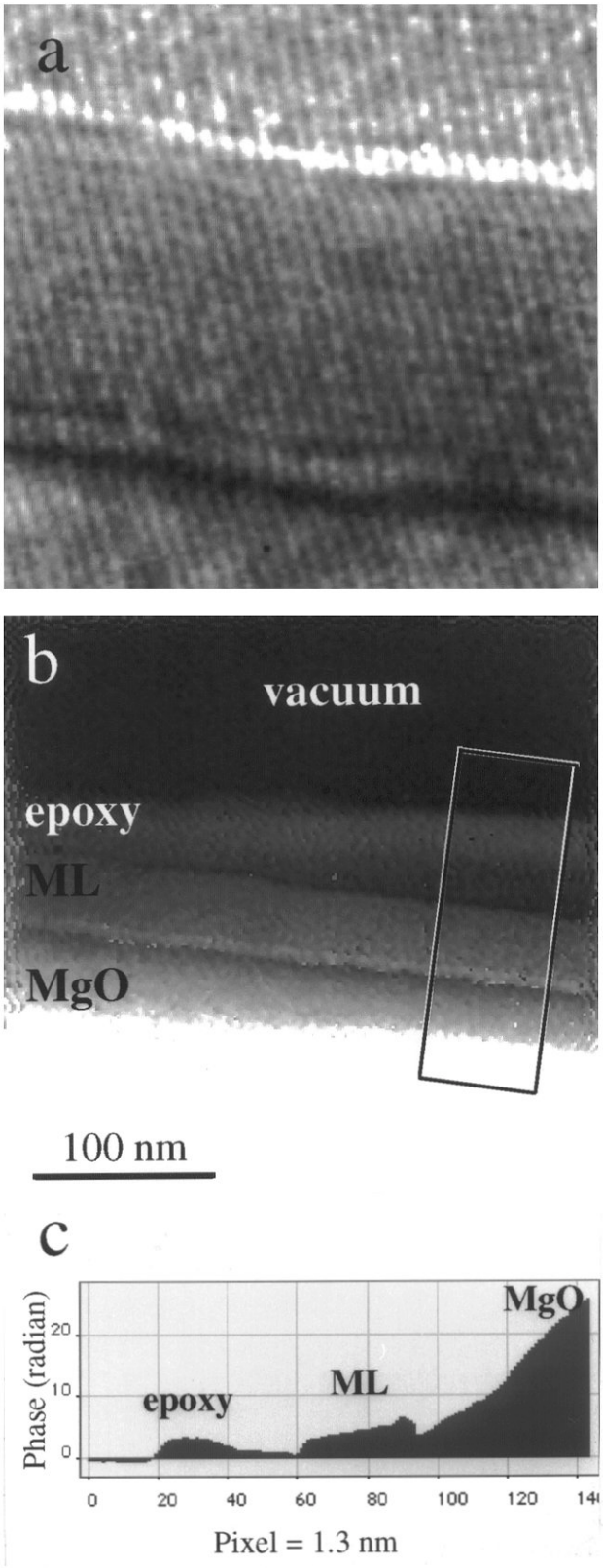

Figure 9. (**a**) detail of hologram of Co/Rh multilayer on MgO substrate; (**b**) reconstructed phase image; (**c**) corresponding line trace from phase image.

hologram in Figure 7c. The lumpiness of the phase shifts in the image is due to both the discontinuous nature of the Co film and the random orientation of the moments of the particles. Figure 8b shows an averaged line trace from the area indicated in Figure 8a. The 16 Co layers can be distinguished.

Co/Rh multilayer

Multilayers consisting of ferromagnetic/non-ferromagnetic metals show great promise as media material because of their huge GMR values (Parkin, 1995). Characterization of their micromagnetic structure, in particular the ferromagnetic or anti-ferromagnetic coupling between layers, is therefore of much interest. Our preliminary cross-sectional observations of an epitaxial Co/Rh multilayer (10 layers of {1.2nm Co | 2.0 nm Rh}) grown by sputtering on MgO(110) illustrates some of the current limitations of electron holography and Lorentz microscopy for studying this type of finely spaced material. Figure 9a shows a section of an electron hologram of the Co/Rh GMR multilayer recorded in cross-section at the highest available electron-optical magnification of the CM200 in the Lorentz lens configuration with the objective lens switched off. A reconstructed phase image is shown in Figure 9b and a line trace across the Co/Rh multilayer is shown in Figure 9c. From careful scrutiny of these various figures, the very existence of the multilayer would appear questionable, and yet it is clearly visible in high magnification images recorded with the objective lens switched on. Why? Consideration of the multilayer dimensions relative to the available magnification, the pixel size of the CCD array, and the requirements for proper sampling of holographic fringes and specimen periodicities (de Ruijter and Weiss, 1993) lead to the conclusion that the hologram is seriously undersampled. With the present configuration of the microscope and detector, it is simply not possible to reconstruct a hologram which gives direct phase information for sample features as small as 2.2 nm.

Discussion

In common with all other electron microscopy techniques, variations in sample thickness complicate quantitative interpretation of reconstructed phase images from off-axis electron holograms. In the case of magnetic samples, where the internal magnetic fields give rise to slopes in the phase image, wedge-shaped samples are predictably problematical because it becomes difficult to separate the effect of the mean inner potential from that due to the magnetic field. Various schemes can be tried to distinguish the two effects including tilting the sample, turning it over, and passing a small current through the objective lens to saturate the film parallel to the electron beam direction. These methods will, however, generate their own additional problems bearing in mind the importance of locating the phase shifts relative to the specimen position and the difficulties associated with alignment of respective pairs of holograms.

It is apparent from the Co/Rh GMR sample that application of off-axis electron holography to finely spaced magnetic multilayers would benefit from alternative phase reconstruction methods. These methods would be especially useful in cases of undersampling when the dimensions of the feature of interest are less than about two or three times the holographic fringe spacing or in regions of large phase gradients when the fringe shifts are large relative to the pixel size, as seen for example in the anisotropic FePt alloy films.

In some situations involving magnetic materials, it must be anticipated that fringing fields will confuse interpretation of the phase images. However, this complication should be revealed by an unacceptable phase curvature in vacuum outside the sample. Such an effect was not visible for the magnetic materials considered in this present study except for the case of the FePt alloy film in Figure 5, where the easy axis was parallel to the film normal.

It became clear during the course of this study that Lorentz microscopy will not be particularly useful for studying micromagnetic fields in ultrafine layers viewed in cross-section, which is contrary to its application to multilayers in the plan-view imaging geometry (Heyderman *et al.*, 1994). The essence of the problem is that Lorentz effects only become visible at large defocus, but such defocus values also imply coarse Fresnel fringes around all features of interest, which will in turn degrade the local resolution and visibility. This degradation goes unnoticed at traditional Lorentz magnifications of 2000-4000x.

Our conclusion from this study is that off-axis electron holography and Lorentz microscopy can play a valuable and often complementary role in characterizing the micromagnetic structure of ultrathin films and multilayers. The combination of techniques should be of valuable when conducting *in situ* studies as a function of specimen temperature and/or the strength of any external applied magnetic field.

Acknowledgements

This work utilized facilities within the Center for High Resolution Electron Microscopy at Arizona State University supported by the National Science Foundation Grant DMR-93-14326. We are grateful to Professor A.E. Berkowitz and Drs. R.F.C. Farrow, S.S.P. Parkin and S.-C.Y. Tsen for their ongoing collaborations and for providing the samples that were described in this work.

References

Chapman JN (1984) The investigation of magnetic domain structures in thin foils by electron microscopy. J Phys D: Appl Phys **17**: 623-634.

Chapman JN, Ferrier RP, Heyderman LJ, McVitie S, Nicholson WAP, Bormans B (1993) Micromagnetics, microstructure and microscopy. Inst Phys Conf Ser **138**: 1-8.

de Ruijter WJ, Weiss JK (1993) Detection limits in quantitative off-axis electron holography. Ultramicroscopy **50**: 269-283.

Farrow RFC, Weller D, Marks RF, Toney MF, Harp GR, Cebollada A (1996) Growth temperature dependence of long-range alloy order and magnetic properties of epitaxial FexPtl-$_x$(x-0.5). J Appl Phys **79**: 1166-1168.

Heyderman LJ, Chapman JN, Parkin SSP (1994) Electron microscope observations of the magnetic structures in magnetoresistive multilayer films. J Phys D: Appl Phys **27**: 881-891.

Lichte H (1991) Electron image plane off-axis holography of atomic structures. In: Advances in Optical and Electron Microscopy, Vol. 12. Mulvey T, Sheppard CJR (eds). Academic Press, New York. pp 25-91.

McFadyen IR, Chapman JN (1992) Electron microscopy of magnetic materials. EMSA Bulletin **22**: 64-75.

McCartney MR, Gajdardziska-Josifovska M (1993) Absolute measurement of normalized thickness, t/λ_i, from off-axis electron holography, Ultramicroscopy **53**: 283-289.

Mul PM, Bormans BJ, Schaap L (1990) Design of a field emission gun for the Philips CM20/STEM microscope. In: Electron Microscopy 1990, Vol. 2. Peachey LD, Williams DB (eds). San Francisco Press, San Francisco. pp 100-101.

Parkin SSP (1995) Giant magnetoresistance in magnetic nanostructures. Ann Rev Mater Sci **25**: 357-388.

Reimer L (1989) Transmission Electron Microscopy. Springer-Verlag, Berlin. p 57.

Tonomura A (1993) Electron Holography. Springer Series in Optical Sciences, Vol. 70. Springer, Heidelberg.

Discussion with Reviewers

S. McVitie: Considering the limitations quoted for reconstruction of sample features is the technique viable for looking at the induction profile of a domain wall?

Authors: Yes, mapping the in-plane induction component is possible, although limits to the accuracy and precision need to be carefully considered. In principle, taking gradients as indicated in Equation (3) will give the induction components if the thickness is known and constant. Complications arise with thickness gradients which will contribute terms proportional to both the mean inner potential and the induction. Fringing fields will also be a problem, although less so than thickness effects as they tend to affect the slope of the phase much more slowly than changes in phase slope near abrupt domain walls. None of the cross-sectional samples shown in these results were suitable for even qualitative induction mapping because of varying thickness profiles. However, hard magnets with abrupt domain walls which can be oriented perpendicular to the film show promise for induction profiling.